ISSN 0029 - 3865

CBPF-NF-028/88.

THE GAP ROAD TO CHAOS AND ITS MAIN CHARACTERISTICS

by

M.C. de Sousa VIEIRA and C. TSALLIS

Centro Brasileiro de Pesquisas Físicas - CBPF/CNPq
Rua Dr. Xavier Sigaud, 150
22290 - Rio de Janeiro, RJ - Brasil

ABSTRACT. We study numerically the three types of asymmetry associated with the map $x' = 1 - \varepsilon_i - a_i |x|^{z_i}$ ($i = 1,2$ respectively correspond to $x > 0$ and $x \leq 0$). The first case is the amplitude asymmetry ($a_1 \neq a_2$), the second case is the exponent asymmetry ($z_1 \neq z_2$) and the last one is a discontinuous map ($\varepsilon_1 \neq \varepsilon_2$). In the two first cases the period-doubling road to chaos is topologically unmodified. In the last case the road to chaos is completely new ("gap road"). Chaos now is attained through sequences of inverse cascades. Various new features are observed, concerning the phase diagram, kneading sequences, Liapunov and uncertainty exponents, number of attractors, multifractality, among others. We also study the crossover between the discontinuous map and the continuous one.

Key-words: Chaos; Dynamical systems; Multifractality; Liapunov Exponent.

1. INTRODUCTION

The evolution of a dynamical system governed by nonlinear one-dimensional difference equation presents a very rich structure[1]. Universal relations in difference equations presenting a single extremum of the $|x|^z$ class ($z>1$) were found by Grossmann and Thomae, Feigenbaum, and Coullet and Tresser[2]. The equation they considered was of the type

$$x_{t+1} = f(x_t) \equiv 1 - a|x_t|^z \qquad (1)$$

The interesting behavior appears for $x_t \in [-1,1]$ and $a \in [0,2]$. For $z = 2$, Eq. (1) is equivalent to the logistic map [$x_{t+1} = 4\mu x_t(1-x_t)$]. When a increses from 0 to $a^*(z)$ [$a^*(2) = 1.401155...$; see ref. 3 for $a^*(z)$] the attractor (or long time solution) of the map (1) exhibits a sequence of periodic orbits with periods 2^k ($k=0,1,2,...$). The sequence $\{a_k\}$ where bifurcations occur, converges geometrically with a rate $\delta_k(z) \equiv (a_k - a_{k-1})/(a_{k+1} - a_k)$, which for large values of k , approaches $\delta(z)$ [$\delta(2) = 4.6692...$; see ref. 3 for other values of z]. Above a^* the chaotic regime appears, where aperiodic attractors are present, as well as an infinite number of periodic windows with period-doubling bifurcations.

After Feigenbaum's work, a great amount of theoretical as well as experimental efforts have been dedicated to study the standard routes to chaos associated with continuous differentiable maps, namely, period-doubling, intermittency and quasiperiodicity. Nevertheless, little effort has been devoted to maps with an asymmetry at the extremum[4-10]. Experimental systems which can be described in terms of asymmetric maps are now appearing (see ref.8 for laser cavity and ref. 9 for nonlinear oscillators). When the singularity is a discontinuity, a new universal scenario to chaos appears[7,10].

The aim of the present paper is to study the following asymmetric map:

$$x_{t+1} = f(x_t) \equiv \begin{cases} 1 - \varepsilon_1 - a_1|x_t|^{z_1} , & \text{if } x_t > 0 \\ 1 - \varepsilon_2 - a_2|x_t|^{z_2} , & \text{if } x_t \leq 0 \end{cases} \qquad (2)$$

The well known continuous symmetric case is recovered for $z_1 = z_2 \equiv z$, $a_1 = a_2 \equiv a$ and $\varepsilon_1 = \varepsilon_2 = 0$. Three types of asymmetry are studied, namely, case I ($a_1 \neq a_2$, $z_1 = z_2 \equiv z$ and $\varepsilon_1 = \varepsilon_2 = 0$), case II ($a_1 = a_2 \equiv a$, $z_1 \neq z_2$ and $\varepsilon_1 = \varepsilon_2 = 0$), and case III ($a_1 = a_2 \equiv a$, $z_1 = z_2 \equiv z$ and $\varepsilon_1 \neq \varepsilon_2$). Some features of these maps such as phase diagrams, attractors, Liapunov and uncertainty exponents, multifractality and others will be studied in the following sections.

2. AMPLITUDE ASYMMETRY (CASE I)

The route to chaos in this case is via period-doubling bifurcations. However, the set $\{\delta_k\}$ asymptotically ($k\to\infty$) presents an oscillatory behavior between two fixed values. Let us now mention at this point that preliminary numerical work[7] suggested that δ_k approaches a single value, namely that of the symmetric case. The present high accuracy calculations show that this is not so, but rather it exhibit the oscillatory behavior, first

studied by Arneodo et al . We have represented in Fig. 1(a) for $z_1 = z_2 = 2$ and $\varepsilon_1 = \varepsilon_2 = 0$, the critical lines [in (a_1,a_2) space] which generalize a^* (the first entrance into chaos) and a^M(value of a above which finite attractors disappear). In Fig. 1(b) we show the limiting values δ_∞ between which $\{\delta_k\}$ oscillates for k large enough; these limiting values are shown as function of a_1 along the critical line $a_2^*(a_1)$ of Fig. 1(a).

3. EXPONENT ASYMMETRY (CASE II)

The route to chaos in this case oncemore is via period-doubling bifurcation. However, a different behavior appears in the set $\{\delta_k\}$: the δ_k's do not converge for incresing k, but proceed in oscillatory fashion between two asymptotic lines (and not limiting values), one of them being divergent[6,7,9]. In Fig. 2 we have presented our results as well as those of ref. 6. This behavior has been recently exhibited experimentally[9]. Above a^* (chaotic region), the relative sizes of the various periodic windows are quite different from those of the $z_1 = z_2$ prototype. However, as in case I, the sequence of high-order windows is the same of the symmetric case, since this map satisfy the conditions required in ref. 11.

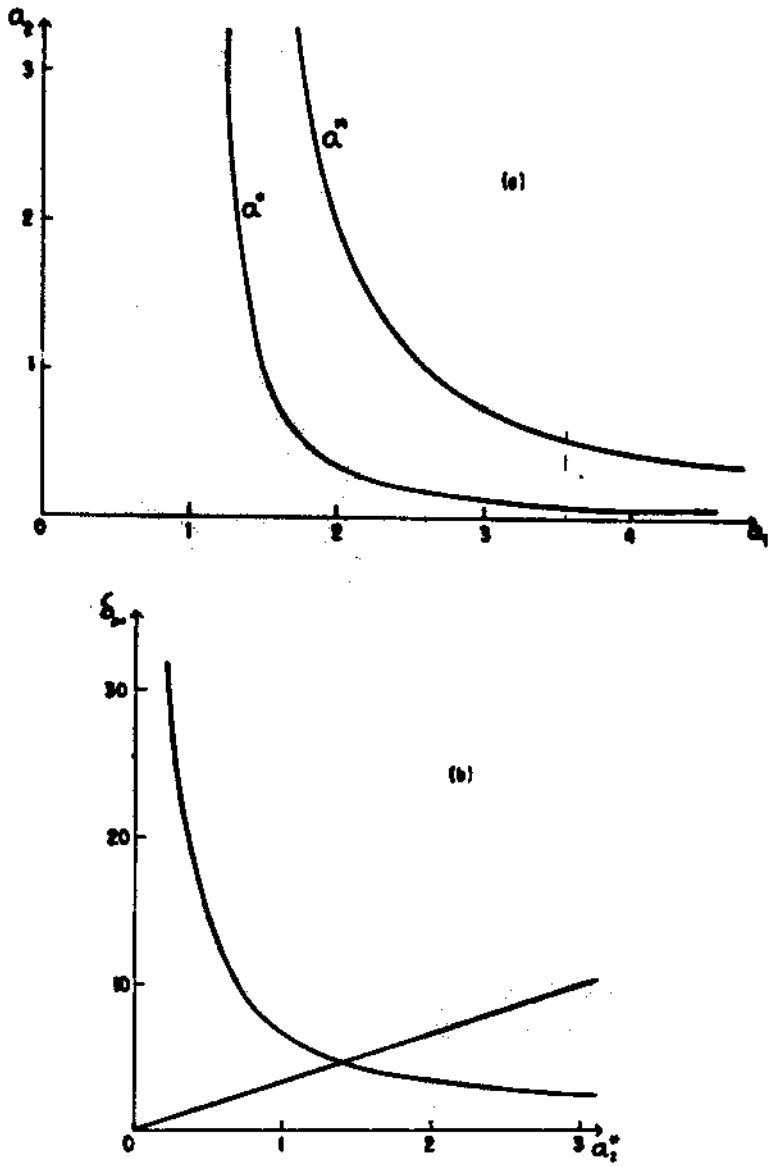

Fig. 1. (a) Special cuts of the "first entrance into chaos" and "finite-attractor-disappearance" hypersurfaces in the (a_1,a_2) space for $z_1 = z_2 = 2$ and $\varepsilon_1 = \varepsilon_2 = 0$; (b) values of δ_k for $k>>1$ as function of a_2 along the critical line $a_2^*(a_1)$ of (a). The numerical results for the asymptotic values are roughly reproduced by $\delta_\infty \cong 3.3a_2^*$ and $\delta_\infty \cong 7/a_2^*$.

4. DISCONTINUOUS MAPS (CASE III)

Maps with a discontinuity at the extremum can be generated, for instance, by appropriate Poincaré sections in flows where trajectories on or near the attractor pass close to a saddle (or hyperbolic) point. In this situation the evolution of the dynamical variable depends on the side with respect to the saddle point, on which the preimages are localized. The standard example of such systems is the Lorenz model, the origin of which

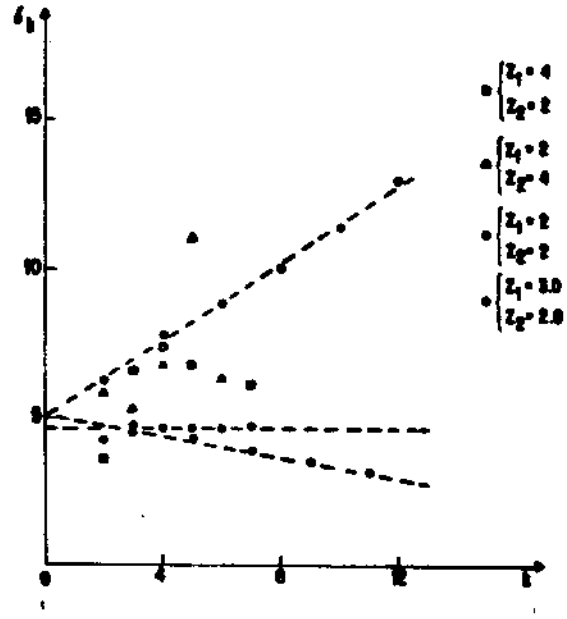

Fig. 2. Evolution of the successive ratios $\{\delta_k\}$ for the $z_1 = z_2 = 2$ prototype and for the case II ($z_1 \neq z_2$).

is a saddle point. A typical map generated on this model is the case III, namely

$$x_{t+1} = f(x_t) \equiv \begin{cases} 1 - \varepsilon_1 - a|x_t|^z, & \text{if } x_t > 0 \\ 1 - \varepsilon_2 - a|x_t|^z, & \text{if } x_t \leq 0 \end{cases} \qquad (3)$$

where $\varepsilon_1 \neq \varepsilon_2$. In ref. 7, it has been indicated that $f(0) = 1 - (\varepsilon_1+\varepsilon_2)/2$, which is not convenient; this choice in fact alters the sequence of inverse cascades. The value of $f(0)$ actually used in the numerical calculations of ref. 7 was $f(0) = 1 - \varepsilon_2$.

4.1. Evolution of the Attractor

A very rich structure is present in the evolution of the attractor. The Fig. 3 shows the a-dependence of the attractor for a typical case, namely $(\varepsilon_1,\varepsilon_2) = (0,0.1)$. We observe the appearance of sequences of inverse cascades in arithmetic progression ("inverse" refers the the fact that a has to decrease in order to approach the accumulation point associated with each cascade) initially mixed with pitchfork bifurcations. The first cascade we observe for increasing a is ...14→12→10→8→6→4, which accumulates on a=1. Immediately above this cascade we observe a couple of standard pitchfork bifurcations. Further on, a new inverse cascade appears as follows: ...21→17→13→9, and then again a pitchfork bifurcation into period 18. Then another inverse cascade appears as follows: ...76→58→40→22. After this cascade, no other standard pitchfork bifurcations are observed (until the entrance into chaos), but instead new inverse cascades are present: ... 70→48→26, and then ... 108→82→56, and then ...142→86→30, etc. A rule is observed: Within each cascade, the periods grow arithmetically by adding the first element immediately below its accumulation point. In

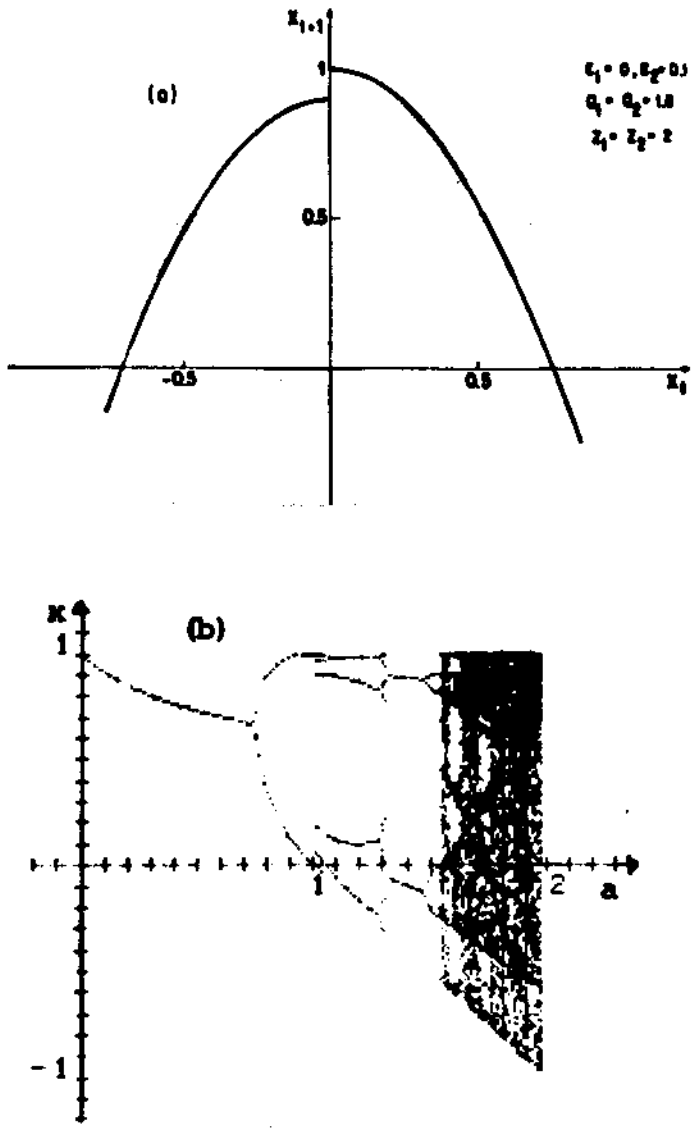

Fig. 3. (a) Discontinuous map and (b) a-evolution of the attractor for $(\varepsilon_1,\varepsilon_2)=(0,0.1)$, $z_1=z_2=2$ and $x_0=0.5$.

fact, we have a very fine structure. We observe that between any two consecutive elements of a cascade there is another inverse cascade whose periods grow with the same rule mentioned above. For example, between the elements 40 and 22 of the third cascade, the cascade ...102→62→22 exists. Between the elements 102 and 62 of this cascade, we have the following one ...266→164→62, and so on. The elements of these cascade appear discontinuously like tangent bifurcations. However, they do not present intermittency, since the iterated function $f(f(...f(x)))$ presents square corners which cross the $f(x)=x$ bissectrix.

In Fig. 4 we have represented, for a typical case, the "phase diagram" in the space of the size of the gap and of a. Such phase diagram will be refered hereafter as bunch of bananas. Initially let us fix ε_1 and vary a. We see the behavior described above: inverse cascades of at-

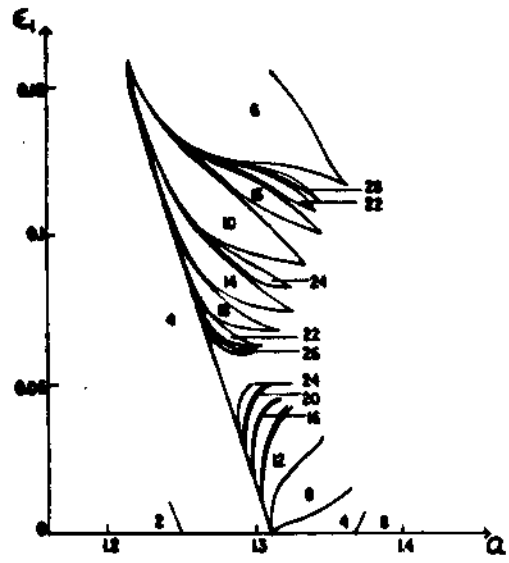

Fig. 4. Phase diagram for $z_1 = z_2 = 2$, $\varepsilon_2 = 0$ and $x_0 = 0.5$. The number indicates the period of the attractor. For $\varepsilon_1 = 0$ we recover the well known period-doubling sequence.

tractors whose periods grow arithmetically and accumulate on values of a, immediately below which appear cycles whose periods precisely are the corresponding adding constants. Furthermore, between any two bananas we always have another banana. The same kind of behavior is observed by fixing a and varying ε_1 (or ε_2, of both, with $\varepsilon_1 \neq \varepsilon_2$). The accumulation points of the cascades in turn accumulate (for increasing a if $(\varepsilon_1,\varepsilon_2)$ are fixed) on a point which is the entrance into chaos. In other words, we have a (presumably) infinite number of accumulation points where there is no chaos (negative Liapunov exponents), as this only emerges at the accumulation point of the accumulation points.

For fixed $(\varepsilon_1,\varepsilon_2)$, a given banana exists between a minimal value a_k^m and a maximal value a_k^M. Within a given cascade of bananas (whose sequence is noted with k = 1,2,3...) , we verify

$$|a_k^m - a_{k+1}^m| \sim |a_{k-1}^m - a_k^m|^{z_1} \qquad (4.a)$$

as well as

$$|a_k^m - a_\infty^m| \sim |a_{k-1}^m - a_\infty^m|^{z_1} \qquad (4.b)$$

for k large enough. The same laws hold for $\{a_k^M\}$, for all values of $(\varepsilon_1,\varepsilon_2)$ such that $\varepsilon_1 \neq \varepsilon_2$, in the presence or absence of higher order terms in Eq. (3). Similar features are observed if we fix a and vary $(\varepsilon_1,\varepsilon_2)$.

4.2. Kneading Sequence

In the windows of the chaotic region for maps governed by (1) there are

different kinds of stable periods of the same length. This differentiation is characterized by the order in which the points are visited. For every periodic orbit, there is one value of the control parameter for which the orbit includes the "critical point" (extremum) of the map. For this value of the control parameter a it is possible to form a word of finite length, by noting whether each of the subsequent iterates in the orbit was less than (to the left: L) or greater than (to the right: R) of the critical point. Thus, a period-3 orbit $x_{crit} \to R \to L \to x_{crit}$, would be uniquely defined by the notation RL which we call the visitation pattern (or kneading sequence). Metropolis, Stein and Stein[11] (see also Derrida et al.[12]) discovered that the order in the arrangement of these words is independent of the unimodal map studied. In particular, if the word P corresponds to a period which actually occurs, we can construct another word $H(P)=P\mu P$, where $\mu=R$ if there is an even number of R's in P and $\mu=L$ otherwise. H is called the harmonic of P and represents the doubled-period adjacent to P.

For the discontinuous maps governed by Eq. (3) the inverse cascades which are observed depend on the size of the gap, as is shown in Fig. 4. For a fixed gap, the construction of the kneading sequences, for a given cascade, obeys the following rule: If P_n is the pattern of the n-cycle that exists immediately below the accumulation point of the cascade and P_k is the pattern of the k-cycle of the cascade, then the pattern of the m-cycle that results form the addition of the n-cycle and of the k-cycle is $P_m=P_k\mu P_n$, where $\mu=R(L)$ if the last bifurcation below that inverse cascade reaches the x=0 axis by $0^+(0^-)$. For instance, in the case $(\varepsilon_1,\varepsilon_2) = (0.1,0)$ when one branch of the attractor with period-4 reaches the $x=0^-$ axis the inverse cascade ...18→14→10 appears (see Fig. 4). The patterns associated with these periods are P_4=RLR, P_{10}=RLRRRLRLR, P_{14}=RLRRRLRLRLRLR $=P_{10}LP_4$, P_{18}=RLRRRLRLRLRLRLRLR=$P_{14}LP_4$, etc. Between the elements 14 and 10 the cascade ...38→24→10 is present. The pattern associated with its elements are $P_{24}=P_{10}LP_{14}$, $P_{38}=P_{24}LP_{14}$, etc.

4.3. Crossover to the Period-doubling Scenario

The number of pitchfork bifurcations in the discontinuous maps is a function of the size of the gap. It increases when the size of the gap decreases, and diverges when the gap vanishes. For example, for $(\varepsilon_1,\varepsilon_2) = (0,0.0001)$ we observe six pitchfork bifurcation (mixtured with inverse cascades), whereas for $(\varepsilon_1,\varepsilon_2) = (0,0.1)$ there are only three pitchfork bifurcations. In the a-evolution of the attractor, a cycle which results from a pitchfork bifurcation can reappear further on: See cycle of size two in Fig. 3. This cycle disappears at the value $a_d = (1-\varepsilon_1)^{1-z_1}$ and reappears at $a_r = (1-\varepsilon_1)/(1-\varepsilon_2)^{z_1}$. To be more precise, these values are slightly modified according to the attractor towards which the system evolves, which in turn depends on the initial condition x_0, as discussed in section 4.5. The reappearance of the cycle with period two can even happen above the first entrance into chaos. For example , the map with $(\varepsilon_1,\varepsilon_2)=(-0.1,0.1)$ first enters into chaos at $a^*\cong 1.23$, whereas $a_r=1.358$. When $\varepsilon_1=\varepsilon_2\equiv\varepsilon$ (continuous map), we have $a_d = a_r = (1-\varepsilon_1)^{1-z_1}$, a fact which clearly illustrates how the crossover to the period-doubling scenario occurs. A similar study can be made for cycles with period 4,8, etc.

4.4. Liapunov Exponent

The chaotic regime is characterized by a high sensitivity on the initial condition (value of x_0). The Liapunov exponent λ provides a quantitative measure of this dependence ($\lambda<0$ and $\lambda>0$ respectively correspond to periodic orbits and to chaotic motion). The Liapunov exponent is defined through

$$\lambda \equiv \lim_{N\to\infty} \frac{1}{N} \sum_{t=0}^{N-1} \ln\left|f'(x)\right|_{x=x_t} \qquad (5)$$

In Fig. 5 we present the a-evolution of the Liapunov exponent for the typical case $(\varepsilon_1,\varepsilon_2) = (0,0.1)$. The first entrance into chaos occurs in this case at $a^* \cong 1.5447414$. We see in Fig. 5 remarkable features: (i) the structure is roughly self-similar; (ii) the "fingers" corresponding to high (low) periods are narrow (large); for a given cascade, they monotonously become narrower when the periods increase and shift towards negative values of λ, thus exhibiting (presumably) infinitely large periods with no chaos; the higest and largest finger of each cascade corresponds to the lowest period of that cascade; if we consider increasingly large lowest periods, the tops of the fingers approach $\lambda=0$ and drive the system into chaos; (iii) changements of periods occur for $\lambda\to-\infty$, in remarkable contrast with changement of periods in the period-doubling road, which occur at $\lambda=0$.

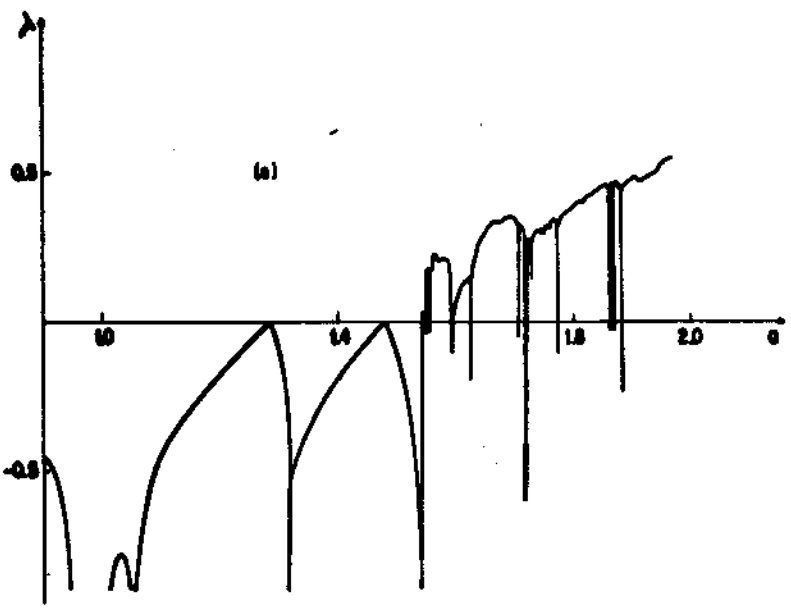

Fig. 5. Evolution of the Liapunov exponent as function of a for $(\varepsilon_1,\varepsilon_2)=(0,0.1)$, $z_1=z_2=2$ and $x_0=0.5$. The numbers in the fingers indicate the period of the attractor (c) is the amplification of the small rectangle in (b), which in turn is an amplification of (a).

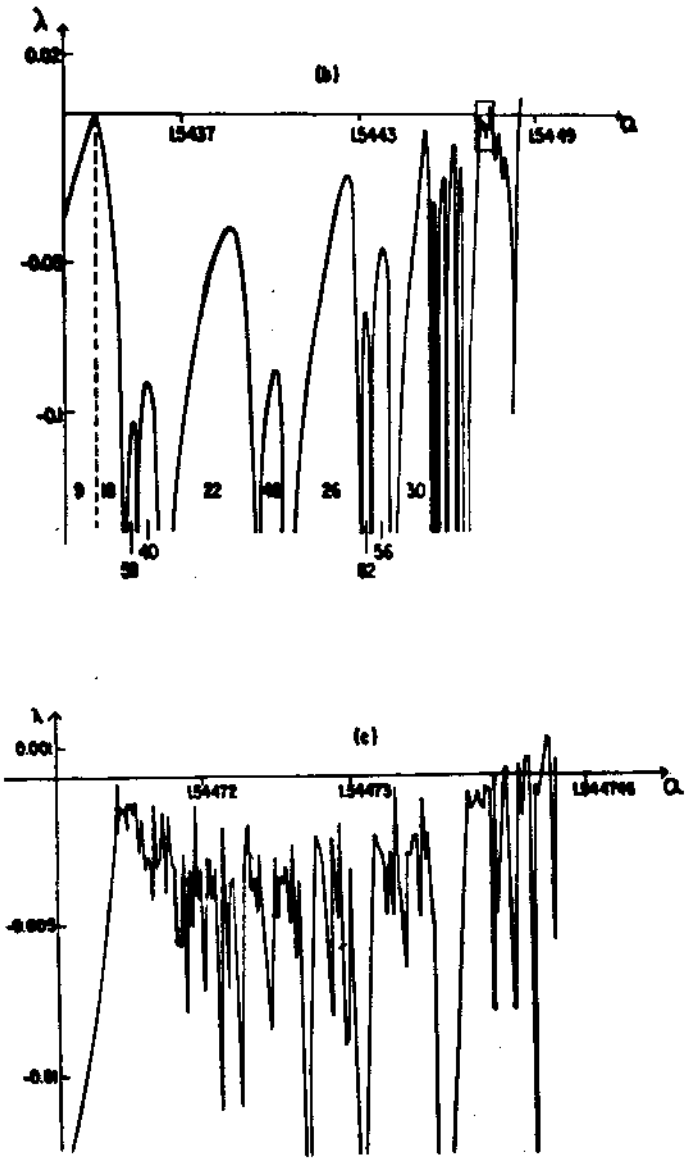

Fig. 5. Continuation.

4.5. Uncertainty Exponent

Continuous one-dimensional maps presenting an unique extremum have at most one finite attractor, which is independent on the initial conditions. In maps with a gap at the extremum we verify that this picture is modified. In such cases, more than one finite attractor (typically two attractors) appear when we cross from one banana (see Fig. 4) to a neighboring one (we made this observation in several crossings, it probably happens in all of them). The attractor which is chosen depends on the

initial value x_0. Two examples are presented in Fig. 6 for a=1.3 and a=1.540344; the black and white regions are euclidean (dimensionality D=1) whereas the border-set between them is a fractal with capacity dimension d. The uncertainty exponent[13] α_u is given by $\alpha_u=D-d$. The system is said to present final-state sensitivity or non-sensitivity according to be $0\leq\alpha_u<1$ or $\alpha_u=1$. To calculate α_u we consider, in the interval of x_0 corresponding to finite attractor (roughly [-1,1])N randomly chosen values (typically $N=10^4$). We then chose ε (say 10^{-3} and below) and check whether both attractors starting from $x_0\pm\varepsilon$ coincide with that of x_0; if not, that value of x_0 is said uncertain. We denote N_u the total number of uncertain points. The uncertainty ratio N_u/N varies as ε^{α_u}. We find $\alpha_u\cong0.85$ ($\alpha_u\cong0.22$) for a=1.3 (a=1.540344). Numerical experiments based on forth and back variations of a might present hysteresis according to the initial value x_0 retained for the various steps (see ref. 10).

Fig. 6. Basins of attraction for typical values of a and $(\varepsilon_1,\varepsilon_2)=(0,0.1)$ and $z_1=z_2=2$. For a=1.3 (a=1.540344) the black and white regions correspond to cycles with period 8 and 2 (25 and 21) respectively.

4.6. Multifractality

The attractor of discontinuous maps at the first entrance into chaos is a multifractal[14]. The formalism used to study multifractals consists in covering the attractor with boxes , indexed by i, of size l_i and assume that the probability density scales like $p_i \propto l_i^{\alpha}$, in the limit $l_i\to0$.The characterization of a multifractal is through the function $f(\alpha)$, which is the dimension of the set of boxes which share a given index α.Through a Legendre transformation, $f(\alpha)$ is related to the generalized dimension D_q[15]. The minimal and maximal values of α respectively coincide with D_∞ and $D_{-\infty}$; the maximal value of $f(\alpha)$ coincides with the Hausdorff dimension D_0. In Fig. 7 we illustrate $f(\alpha)$ for the case $(\varepsilon_1,\varepsilon_2)=(0,0.1)$. Its shape is different (more square-like) from that obtained without gap (period-doubling road to chaos), and the values we obtain are $D_0\cong0.95$, $D_\infty\cong0.45$ and $D_{-\infty}\cong5.7$. Notice that the period-doubling relation $D_{-\infty}=zD_\infty$ fails in the gap case.

4.7. Discontinuous map as a limit case

Since physical maps presumably do not exhibit a (sharp) discontinuity,

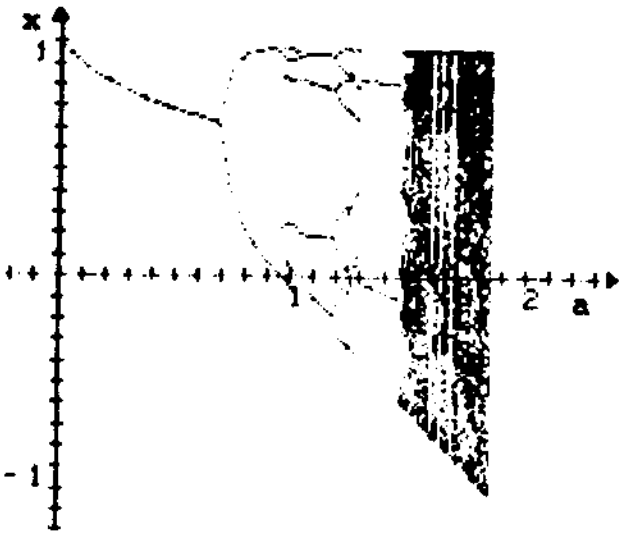

Fig. 8. Evolution of the attractor as a function of a for the equation (6) with ε=0.1, w=0.1 , z=2 and x_0=0.5.

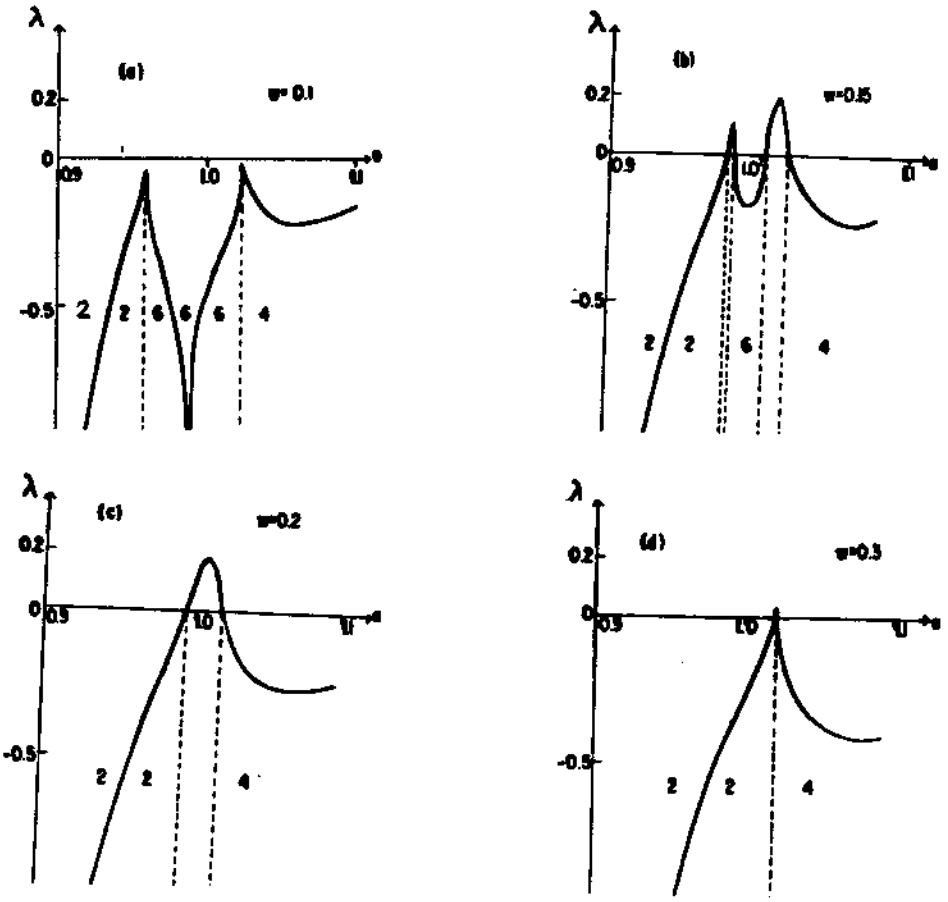

Fig. 9. Liapunov exponent as a function of a for ε=0.1, z=2, x_0=0.5 and w=0.1, 0.15, 0.2, 0.3. The numbers indicate the period of the attractor.

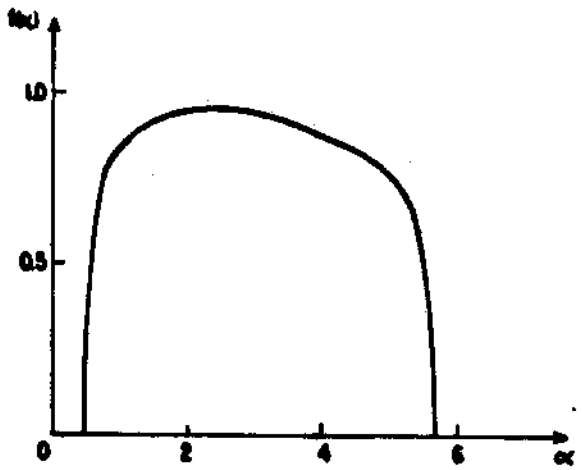

Fig. 7. Multifractal funtion $f(\alpha)$ for $(\varepsilon_1,\varepsilon_2)=(0,0.1)$, $z_1=z_2=2$ and $x_0=0.5$ (chaos appears at $a^*\cong 1.5447414$).

we consider in this section the following continuous map[16]

$$x_{t+1} = f(x_t) \equiv 1 + \varepsilon|x|^w \mathrm{sgn}(x) - a|x|^z \qquad (6)$$

with $w<1<z$. When $w<<1$ this map has a general shape very similar to the map (1), but without discontinuities. In the case $w=0$, the rapidly changing part of $f(x)$ around $x=0$ is replaced by a jump, and we recover the discontinuous map (with $\varepsilon_1=\varepsilon_2\equiv\varepsilon$). Notice that the map (6) has a Schwarzian derivative which is positive for an interval of x around $x=0$. In Fig. 8 we show the a-evolution of the attractor for a typical case. This picture is roughly similar to Fig. 3. Near $a=1$ we observe the cycles with periods $2\to6\to4$, a fact which is a reminiscence of the inverse cascade $2\ldots10\to8\to6\to4$. When w increases the map becomes more and more similar to the logistic map (Eq. (1)), therefore a crossover to the period-doubling scenario is expected. In Fig. 9 we show this crossover for a particular range of a. Initially, we observe that both extrema correponding to changement of periods $2\to6$ and $6\to4$become chaotic and then merge in one extremum and then becomes chaotic again.

For $\varepsilon>0$ we found, in all cases studied, a sudden entrance into chaos when the external parameter a is varied. For $\varepsilon<0$ we found, before the first entrance into chaos, a sequence of period doubling bifurcations with the convergence ratio of the set $\{\delta_k\}$ being approximately the same of the logistic equation. Therefore we observe indications for a route to chaos via period-doubling in maps with positive Schwarzian derivative for an interval of x around $x=0$. This situation is unusual and seems to us an interesting question, worthy to be studied, since the maps studied until now that present period-doubling route to chaos have negative Schwarzian derivative for <u>all</u> finite values of the dynamical variable.

5. CONCLUSIONS

We have shown that an asymmetry introduced in the logistic map can alter some of its basic features. Amplitude asymmetry ($a_1 \neq a_2$) and exponent asymmetry ($z_1 \neq z_2$) do not alter the bifurcation sequence, but the unique tendency associated with the set $\{\delta_k\}$ disappears. In the discontinuous map ($\epsilon_1 \neq \epsilon_2$) the route to chaos is completely modified. Sequences of inverse cascades in arithmetic progression are observed in the evolution of the attractor. There is no chaos at the accumulation point of these cascades, which appears only at the accumulation point of the accumulation points. Several other unusual features were found at the phase diagram, Liapunov and uncertainty exponents, multifractality, among others.

We acknowledge with pleasure very fruitful suggestions by H.W. Capel, M. Napiórkowski, as well as interesting remarks by A. Coniglio, E.M.F. Curado, H.J. Herrmann, J.P. van der Weele and Ph. Nozières. We are indebted to P. Coullet and C. Tresser for calling our attention on ref. 4.

REFERENCES

1. R.M. May, Nature **261**, 459 (1976).
2. S. Grossmann and S. Thomae, Z. Naturf. **32A**, 1353 (1977); M.J. Feigenbaum, J. Stat. Phys. **19**, 25 (1978); P. Coullet and C. Tresser, J. Phys. (Paris) Colloq. 5, C25 (1978).
3. P.R. Hauser, C. Tsallis and E.M.F. Curado, Phys. Rev. A **30**, 2074 (1984). Bambi Hu and Indubala I. Satija, Phys. Lett. **98A**, 143 (1983); J. P. Eckmann and P. Wittwer, Computer Methods and Borel Summability Applied to Feigenbaum's Equation, Lectures Notes in Physics, vol. 227 (Springer, Berlin, 1985); J.P. van der Weele, H.W. Capel and R. Kluiving, Phys. Lett. **119A**, 15 (1986); J.K. Bhattacharjee and K. Banerjee, J. Phys. A **20**, L269 (1987); M.O. Magnasco and D.L. Gonzalez, private communication; M.C. de Sousa Vieira, unpublished.
4. A. Arneodo, P. Coullet and C. Tresser, Phys. Lett. **70A**, 74 (1979).
5. P. Szépfalusy and T. Tél, Physica **16D**, 252 (1985); J.M. Gambaudo, I. Procaccia, S. Thomae and C. Tresser, Phys. Rev. Lett. **57**, 925 (1986).
6. R.V. Jensen and L.K.H. Ma, Phys. Rev. A **31**, 3993 (1985).
7. M.C. de Sousa Vieira, E. Lazo and C. Tsallis, Phys. Rev. A **35**, 945 (1987).
8. A.A. Hnilo, Optics Commun. **53**, 194 (1985); A.A. Hnilo and M.C. de Sousa Vieira, J. Opt. Soc. Am., in press.
9. M. Octavio, A, Da Costa and J. Aponte, Phys. Rev. A **34**, 1512 (1986).
10. M.C. de Sousa Vieira and C. Tsallis, unpublished; M.C. de Sousa Vieira and C. Tsallis, to appear in Disordered Systems in Biological Models, eds. L. Peliti and S.A. Solla (World Scentific, 1988); M.C. de Sousa Vieira and C. Tsallis, to appear in Universalities in Condensed Matter, eds. R. Jullien, L. Peliti, R. Rammal and N. Boccara (Springer Proc. Phys.,1988)
11. M. Metropolis, M.L. Stein and P.R. Stein, J. Combinatorial Theory A **15**, 25 (1973).
12. B. Derrida, A. Gervois and Y. Pomeau, J. Phys. A **12**, 269 (1979).

13. C. Grebogi, S.W. McDonald, E. Ott and J.A. Yorke, Phys. Lett. 99A, 415 (1983); M. Napiórkowski, Phys. Lett. 113A, 111 (1985).
14. T.C. Halsey, M.H. Jensen, L.P. Kadanoff, I. Procaccia, and B.I. Shraiman, Phys. Rev. A 33, 1141 (1986).
15. H.G.E. Hentschel and I. Procaccia, Physica 8D, 435 (1983).
16. Z. Kaufmann, P. Szépfalusy and T. Tél, unpublished.